ROLE OF SINGLE-CHANNEL STOCHASTIC NOISE ON BURSTING CLUSTERS OF PANCREATIC β-CELLS

T. REE CHAY AND HONG SEOK KANG
Department of Biological Sciences, University of Pittsburgh, Pittsburgh, Pennsylvania 15260

ABSTRACT To study why pancreatic β-cells prefer to burst as a multi-cellular complex, we have formulated a stochastic model for bursting clusters of excitable cells. Our model incorporated a delayed rectifier K^+ channel, a fast voltage-gated Ca^{2+} channel, and a slow Ca_i-blockable Ca^{2+} channel. The fraction of ATP-sensitive K^+ channels that may still be active in the bursting regime was included in the model as a leak current. We then developed an efficient method for simulating an ionic current component of an excitable cell that contains several thousands of channels opening simultaneoulsy under unclamped voltage. Single channel open–close stochastic events were incorporated into the model by use of binomially distributed random numbers. Our simulations revealed that in an isolated β-cell $[Ca^{2+}]_i$ oscillates with a small amplitude about a low $[Ca^{2+}]_i$. However, in a large cluster of tightly coupled cells, stable bursts develop, and $[Ca^{2+}]_i$ oscillates with a larger amplitude about a higher $[Ca^{2+}]_i$. This may explain why single β-cells do not burst and also do not release insulin.

I. INTRODUCTION

The pancreatic β-cell is responsible for insulin secretion from the islets of Langerhans. In response to glucose, the β-cell exhibits interesting electrical bursting patterns. Although the exact mechanism of the glucose response is not yet clear, there are several properties which are well established. In the absence of glucose, the ATP-blockable K^+ channels control the membrane potential. Upon addition of glucose, these channels are blocked and the β-cell depolarizes. The membrane potential then oscillates between -55 mV (referred to as the silent phase) and -35 mV (the plateau phase). Fast spikes appear on the top of the plateau phase. Under steady-state glucose stimulation, slow waves and bursts occur in regular intervals in electrical recordings from whole islets, but spikes occur rather chaotically (Bangham et al, 1986; Soria and Ferrer, 1986). The durations of the silent and plateau phases are altered by the glucose concentration.

The β-cells within the same islet are known to be strongly coupled and burst regularly with the same frequency (Eddlestone, 1984; Meda et al., 1984). When cells are isolated, however, it is quite difficult and sometimes even impossible to faithfully record membrane potential from single cells (Rorsman and Trube, 1986). In isolated cells, the opening or closing of channels has an important influence on the membrane potential. As a consequence of the stochastic noise, the cells may not produce bursts. Irregular bursts can be observed in a cluster of 70 μm diameter (Rorsman and Trube, 1986). The fact that β-cells in an islet are tightly coupled and produce regular bursts raises interesting questions. What is the advantage of the cells working as a unit? Could coupled cells secrete more insulin than single cells? That is, does stable bursting give rise to an increase in $[Ca^{2+}]_i$? It is not yet feasible to correlate experimentally $[Ca^{2+}]_i$ levels with cluster sizes.

In recent years, patch-clamp recordings have greatly enhanced our understanding of the properties of ionic channels in many excitable cells. New experimental evidence indicates that the Ca_i-activated K^+ channel does not play a major role in bursting (Cook et al., 1984; Kramer and Zucker, 1985; Rorsman and Trube, 1986). Using the whole-cell patch-clamp method, Rorsman and Trube (1986) have characterized a delayed Ca_i-insensitive K^+ channel and a voltage-gated Ca^{2+} channel that play the key roles in the bursting of NMRI mice β-cells. Satin and Cook (1988) have demonstrated the coexistence of low- and high-threshold voltage-activated Ca^{2+} channels in insulin-secreting HIT cells and neonatal rat cells. Since the kinetics of the two channels are very similar and, moreover, the two threshold potentials are close, they had some difficulty in separating the two channels (Satin and Cook, 1988). Identification of two functionally different Ca^{2+} channels is essential in sorting out their cellular functions (Cook, 1984).

The whole-cell voltage-clamp experiments on β-cells (Satin and Cook, 1985 and 1988; Findlay and Dunne, 1985; Rorsman and Trube, 1986) have provided a basis for formulating a better mathematical model. We have recently formulated a model based on these experimental findings (Chay, 1987; Chay and Kang, 1987; Chay and Cook, 1988). This model differs from our earlier ones (Chay and Keizer, 1983; Chay, 1986) in that the termination of spikes and bursts is due to the inactivation of Ca^{2+} channel by intracellular calcium ions (Kramer and Zucker, 1985). In our earlier model (Chay, 1986), a voltage-

gated, Ca_i-sensitive K^+ channel plays the dual role of generating a pacemaker current as well as the spikes. But, in our more recent model, the Ca_i-sensitive K^+ channel is not operative in the bursting regime, and a voltage-gated Ca^{2+} channel (that contains two voltage activated gates, i.e., a high-threshold gate and a low-threshold gate that is blockable by intracellular Ca^{2+} ions) takes over the role of the K-Ca channel (Chay, 1987; Chay and Kang, 1987). In the model of Chay and Cook (1988), we have incorporated two functionally different Ca^{2+} channels: a high-threshold fast channel and a low-threshold slow channel that is blockable by intracellular Ca^{2+} ions (for a review, see Chay, 1988). All these models are, however, deterministic and are not applicable to a cell containing a finite number of channels. Thus, it is our intent to extend our deterministic models to more general stochastic models.

The outline of this paper is as follows. In section II, we will formulate a stochastic model which is applicable to single cells containing a finite number of channels, and in section III we will develop an efficient method of simulating spontaneous voltage fluctuations from a cluster of excitable cells. In section IV, we will apply the method to β-cell clusters to study the effect of the size of β-cell clusters on voltage fluctuations. Specifically, we will study the role of stochastic noise on $[Ca^{2+}]_i$ levels and a lower limit for the number of interconnected cells in a pacemaker group which exhibits a regular firing pattern. In addition, we attempt to sort out the role of the two calcium currents by simulating the whole-cell voltage-clamp experiments (i.e., current traces and I/V plots).

II. STOCHASTIC MODEL

Let us consider a three-dimensional array of excitable cells contacting through a junctional membrane. Cells are allowed to communicate through gap junctions, where the junction is modeled as a resistor. The membrane potential $V^{(j)}$ of the jth cell in such a multicellular complex can be computed from a cable model (Plonsey and Fleming, 1969), where a capacitance is connected in parallel to ionic channels, and the cells are connected in series by a conductance g_g:

$$g_g \nabla^2 V^{(j)} = \Sigma_i I_i^{(j)} + 4\pi r^2 C_m dV^{(j)}/dt. \quad (1)$$

Here, C_m is the membrane capacitance, and r the radius of a cell. Note that if $g_g = 0$, the above equation reduces to a single cell voltage equation. Note also that if g_g is very large (i.e., infinity), then all M cells discharge virtually simultaneously. Thus, a complex consisting of M cells may be considered as one pacemaker cell with the surface area increased by a factor M and the number of channels increased by the same factor.

The components of the membrane ionic current in Eq. 1 are defined by a given model. The excitable cell model that is considered in this work contains (*a*) a delayed rectifier K^+ current $I_{K,V}$, (*b*) a fast voltage–activated Ca^{2+} current $I_{Ca,f}$, (*c*) a slow Ca^{2+} current $I_{Ca,s}$, and (*d*) a leak current I_L that includes contributions from the electrogenic pump current, exchanger current, and possibly the ATP-blockable K^+ current. Thus, according to the Hodgkin-Huxley model (1952) the equation which describes the membrane potential for our model is

$$-4\pi r^2 dV/dt = I_{K,V} + I_{Ca,f} + I_{Ca,s} + I_L, \quad (2)$$

where the explicit expression of each ionic component is given in Table I. We note that our model differs from the Chay-Cook model (1988) in that we have replaced the linearity in $I(V)$ by the Goldman-Hodgkin-Katz equation (Goldman, 1943). The deviation from the linearity comes in only when the membrane potential is more depolarized than the "spiking" potential (i.e., > -10 mV), and thus this replacement affects little on β-cell bursting. The Goldman-Hodgkin-Katz equation, however, is needed in obtaining the inward rectification shown in Fig. 1. Also, the gating variable of the slow calcium channel is separated into a voltage-gated activation term s and Ca_i-blockable inactivation term h of the form (Eckert and Chad, 1984),

$$h = 1/(1 + [Ca^{2+}]_i/K_s), \quad (3)$$

TABLE I

Delayed rectifier K^+ current: $I_{K,V} = n\,\bar{I}_{K,V}$,

where $\bar{I}_{K,V} = P_{K,V}\left(\frac{FV}{RT}\right)\frac{[K^+]_o - [K^+]_i\, e^{FV/RT}}{1 - e^{FV/RT}}$.

$P_{K,V} = 1.3$ pA · mM^{-1}; $[K^+]_o = 5$ mM; $[K^+]_i = 130$ mM.
$\alpha_n = \lambda_n \exp[(V - V_n)/S_n]$; $\beta_n = \lambda_n$.
$V_n = -10$ mV; $S_n = 6$ mV; $\lambda_n = 0.05$ ms^{-1}.

Fast Ca^{2+} current: $I_{f,Ca} = m\,\bar{I}_{f,Ca}$,

where $\bar{I}_{Ca,f} = P_{Ca,f}\left(\frac{2FV}{RT}\right)\frac{[Ca^{2+}]_o - [Ca^{2+}]_i\, e^{2FV/RT}}{1 - e^{2FV/RT}}$.

$P_{Ca,f} = 8.0$ pA · mM^{-1}; $[Ca^{2+}]_o = 3.0$ mM.
$\alpha_m = \lambda_m \exp[(V - V_m)/2S_m]$; $\beta_m = \lambda_m \exp[(V_m - V)/2S_m]$.
$V_m = -13$ mV; $S_m = 8$ mV; $\lambda_m = 0.2$ ms^{-1}.

Slow Ca^{2+} current: $I_{Ca,s} = s\,h\,\bar{I}_{Ca,s}$,

where $\bar{I}_{Ca,s} = P_{Ca,s}\left(\frac{2FV}{RT}\right)\frac{[Ca^{2+}]_o - [Ca^{2+}]_i\, e^{2FV/RT}}{1 - e^{2FV/RT}}$.

$P_{Ca,s} = 2.7$ pA · mM^{-1}; $[Ca^{2+}]_o = 3.0$ mM.
$\alpha_s = \lambda_s \exp[(V - V_s)/2S_s]$; $\beta_s = \lambda_s \exp[(V_s - V)/2S_s]$.
$V_s = -35$ mV; $S_s = 8$ mV; $\lambda_s = 0.2$ ms^{-1}.
$h = h_\infty = 1/(1 + [Ca^{2+}]_i/K_s)$; $K_s = 100$ nM

Leak current: $I_L = g_L(V - V_L)$,
where $g_L = 200$ pS; $V_L = -58$ mV.

Other parametric values are: $f = 0.001$, $k_{Cs} = 0.05$ms^{-1}, $r = 6$ μm, $C_m = 1$ μF · cm^{-2}, and $RT/F = 26.7$ mV. The permeability coefficient expressed in the unit of A · mM^{-1} in the table can be converted to a more familiar unit in meters per second using the conversion factors, 1 A · mM^{-1} = 1 J · V^{-1} · mol^{-1} · m^3 · s^{-1} and $4\pi r^2 F = 4.5 \times 10^{-5}$ J · V^{-1} · mol^{-1} · m^2.

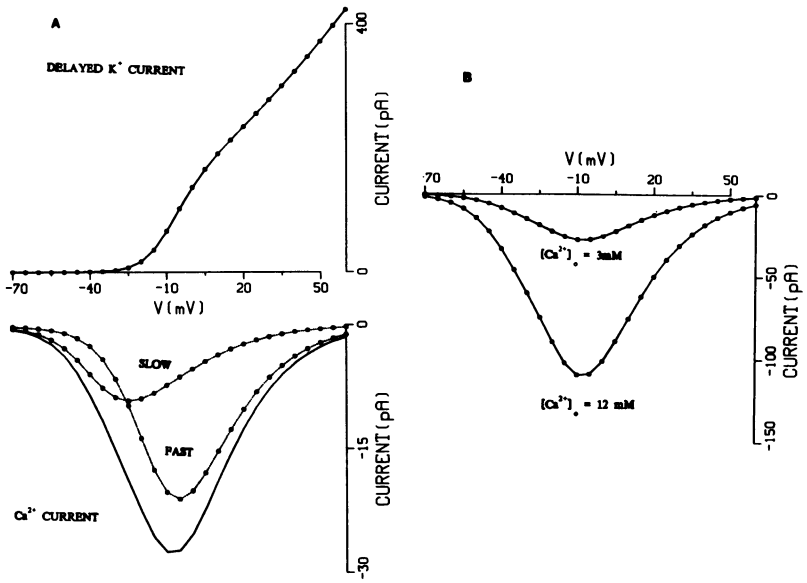

FIGURE 1 (*A*) Peak current-voltage relations elicited by voltage commands from a holding potential of −70 mV. Here, the outward (*top*) current is the delayed K^+ current, and the inward (*bottom*) current is the combined inward current of fast and slow Ca^{2+} currents. (*B*) Peak current-voltage of total inward current in two different external calcium concentrations, i.e., 3 and 12 mM.

where K_s is the dissociation constant of Ca_i ions from the receptor site of the slow calcium channel. In the Chay-Cook model, I_{Ca} has a voltage-dependent gating variable s, whose half maximal potential V_s shifts to the right on the voltage-axis as $[Ca^{2+}]_i$ increases.

In our model, the Ca_i-blockable Ca^{2+} current has a slowly varying component owing to slow changes in $[Ca^{2+}]_i$. This change is due to the influx of extracellular calcium ions through the voltage-gated calcium channel and the efflux of free intracellular Ca^{2+} ions by the action of Ca-ATPase pump activity. Thus, in the limit cycle we may express the dynamical change of $[Ca^{2+}]_i$ by

$$f^{-1}\mathrm{d}[Ca^{2+}]_i/\mathrm{d}t = -(I_{Ca,f} + I_{Ca,s})/2Fv - k_{Ca}[Ca^{2+}]_i, \quad (4)$$

where F is the Faraday constant, f a measure the fraction of free calcium ions in the cell, v the volume of the cell (i.e., $4\pi r^3/3$), and k_{Ca} the rate constant for the efflux of Ca_i. We note that during the initial transient period, the efflux of Ca_i is also due to sequestration of $[Ca^{2+}]_i$ by the intracellular compartments (e.g., mitochondria). Sequestration, however, ceases to exist after 10 min or so. Thus, in the limit cycle steady state, the efflux of Ca_i would mainly be Ca-ATPase actively pumping Ca_i ions out of the cell.

As shown in the two tables, the general form of the time- and voltage-dependent current component of the y-type channel has the form

$$I_y = p_y N_y i_y = p_y \bar{I}_y, \quad (5)$$

where p_y is the fraction of channels open at time t, i_y is the unitary current, and N_y is the total number of channels, and $\bar{I}_y$ is the maximal current per cell. The subscript y stands for one of the three (delayed K^+, fast Ca^{2+}, and slow Ca^{2+}) channels. The maximal currents for three components are given in Table I, where P_y is the "maximal" permeability coefficient of the y-type ions, and $[Y^{Z+}]_o$ and $[Y^{Z+}]_i$ are the extracellular and intracellular concentrations, respectively, of y-type ions carrying charge Z^+. For the sake of clarity, we will drop the subscript y in the ensuing discussion.

If the number of channels, N, is finite, the fraction, p, of open channels is stochastic and cannot be determined uniquely. As N becomes very large, however, the distribution of p is approximately normal (according to the Central Limit Theorem) with mean $\langle p \rangle$ and variance $\langle p \rangle(1 - \langle p \rangle)/N$. Because the standard deviation of the distribution of p is inversely proportional to $\sqrt{N}$, the width of the p distribution becomes narrower and narrower as N approaches ∞. Finally, the distribution becomes a delta function in the limit $N \to \infty$, i.e., p takes on its mean value $\langle p \rangle$. If p stands for n, m, or s in Table I, then $\langle p \rangle$ can be determined uniquely from the following differential equation.

$$\mathrm{d}\langle p \rangle/\mathrm{d}t = (p_\infty - \langle p \rangle)/\tau$$
$$p_\infty = 1/[1 + \exp((V_{1/2} - V)/S)]$$
$$\tau = 1/(\alpha + \beta), \quad (6)$$

where S is the slope of the Boltzmann curve at the half-maximal potential $V_{1/2}$, and α and β are the activation and deactivation rate constants, respectively (see Table I for the expressions of α and β).

It should be emphasized here that Eq. 6 is applicable to a cell containing an infinite number of channels or a cluster containing a large number of strongly coupled cells, such as cells in an islet. If a cell contains only a finite number of channels, p is a random variable and is defined by

$$p(t) = N_O(t)/N, \quad (7)$$

where $N_O(t)$ is the number of open channels at time t. Thus, to determine $p(t)$ we require the number of open

channels $N_O(t)$ at time t, where $N_O(t)$ must be a random variable. In the next section, we develop a method of determining $N_O(t)$ with the random number generators in commercially available mathematical/statistical libraries.

III. GENERATING THE NUMBER OF CHANNELS IN THE OPEN STATE, $N_O(t)$

In this section, we develop an efficient method of simulating the ionic current component I_y of an excitable cell containing several thousand channels under an unclamped condition. To begin our development, let a channel open and close by simple first order kinetics:

$$\text{C (closed)} \underset{\beta}{\overset{\alpha}{\rightleftharpoons}} \text{O (open)}, \tag{8}$$

where C and O are the closed and open states. If the channel is in state O at time t, then in time Δt it will either make a transition to state C or stay in O. The probability of making such a transition to the closed state is given by $\beta\Delta t$.

Let $P_{i,j}$ be the probability that the channel in state i goes to a new state j in Δt and let $P_{i,j}$ be the probability that the channel remains in state i during the interval Δt. Then these probabilities are related to the rate constants in Eq. 7 by

$$\begin{aligned} P_{C,O} &= \alpha\Delta t \qquad P_{C,C} = 1 - \alpha\Delta t \\ P_{O,C} &= \beta\Delta t \qquad P_{O,O} = 1 - \beta\Delta t. \end{aligned} \tag{9}$$

Let there be $N_i(t)$ channels in state i at time t. The number of channels which will be in state O at time $t + \Delta t$ is the sum of the channels which would make a transition from C to O and those which will stay in O during the time interval Δt. In other words,

$$N_O(t + \Delta t) = N_{C,O} + N_{O,O}, \tag{10}$$

where $N_{i,j}$ is the number of channels which will go to state j from state i during the time interval Δt. Since the total number of channels N is fixed, the number of channels in the closed state at $t + \Delta t$ must be equal to

$$N_C(t + \Delta t) = N - N_O(t + \Delta t). \tag{11}$$

A question then is how to determine $N_{i,j}$. During the interval Δt, the number of channels which will go to state j from state i is any number between 1 and N_i with the probability of success being $P_{i,j}$ (see Eq. 9). To find out how many channels would go to the new state j in the next time interval, we have to carry out a series of "coin-tossing" experiments. Fortunately, this experiment can be done conveniently by using one of the binomial random number generators in standard mathematical and statistical libraries (e.g., International Mathematical and Statistical Library [IMSL]). To use such a generator, we need information on the probability of success (i.e., $P_{i,j}$) and the number of trials (i.e., N_i). In particular, if we are using IMSL (version 9), the subroutine

$$\text{GGBN(DSEED, NR, NIND, P, IR)} \tag{12}$$

should be used to determine $N_{C,O}$ and $N_{O,O}$. Here, NR is the number of binomial random deviates to be generated (in our case NR = 1), and DSEED is an input/output double precision variable assigned an integer value (e.g., DSEED = 123457D0 supplied by a user) and replaced automatically by a new value to be used in a subsequent call. If we are calling this routine to determine $N_{C,O}$, P stands for $P_{C,O}$, NIND for $N_C(t)$, and IR for $N_{C,O}$. If it is for $N_{O,O}$, P stands for $P_{O,O}$, NIND for $N_O(t)$, and IR for $N_{O,O}$. (For a newer vectorized version of IMSL, the reader should refer to the subroutine RNMTN, a general multinomial random number generator in IMSL version 10).

It is informative to mention here that as N becomes very large, a binomial distribution becomes Poisson or Gaussian. In particular, it is Poisson if either $\langle p \rangle \cdot N_i$ or $(1 - \langle p \rangle) \cdot N_i$ is of moderate magnitude (Feller, 1968). Otherwise, binomial becomes Gaussian. Although it is always proper to use a binomial distribution in a two-state stochastic process, a binomial distribution becomes computationally unfeasible as N becomes large, and thus it is necessary to use the approximation. The fact that the binomial random number generator in IMSL works for large N must mean that the approximation as mentioned above had already been built into the subroutine.

With the method outlined above, the ionic current at time t can be obtained by a time-discretization recursive method. That is, $I(t)$ at $t + \Delta t$ can be computed iteratively starting from $p(t)$ at time zero (i.e., p_∞ at the resting potential). The size of Δt is constrained by the fact that all the $P_{i,j}$s in Eq. 9 should be between zero and unity. It is sufficient to choose the Δt value to be one-tenth smaller than the inverse of the largest rate constant among αs and βs. Because some of the $p(t)$s are functions of V as well as $[Ca^{2+}]_i$, we obtain V using Eq. 2 and $[Ca^{2+}]_i$ using Eq. 4 with a two-time step Euler method.

IV. SIMULATIONS

The stochastic model given in Table I and the method presented in section III are the basis for the numerical simulations. The differential equations, Eqs. 2 and 4, were solved numerically by a two-time step Euler method. The Cray X-MP/48 at the Pittsburgh Supercomputing Center was used to carry out the computations. To obtain $N_O(t)$ we used the routine GGBN (binomial random number generator) in the IMSL library, but to cross-check our results we also used GGNQF (Gaussian random numbers generator) in the same library. The parametric values used for the computation are listed in Table I. The V_m, V_s, S_m, and S_s values were obtained by fitting the I_{Ca}/V curve of Rorsman and Trube (1986) with our two combined calcium currents as closely as possible. The Rorsman and Trube value of V_n (i.e., -19 mV) with a smaller $P_{K,V}$ gave

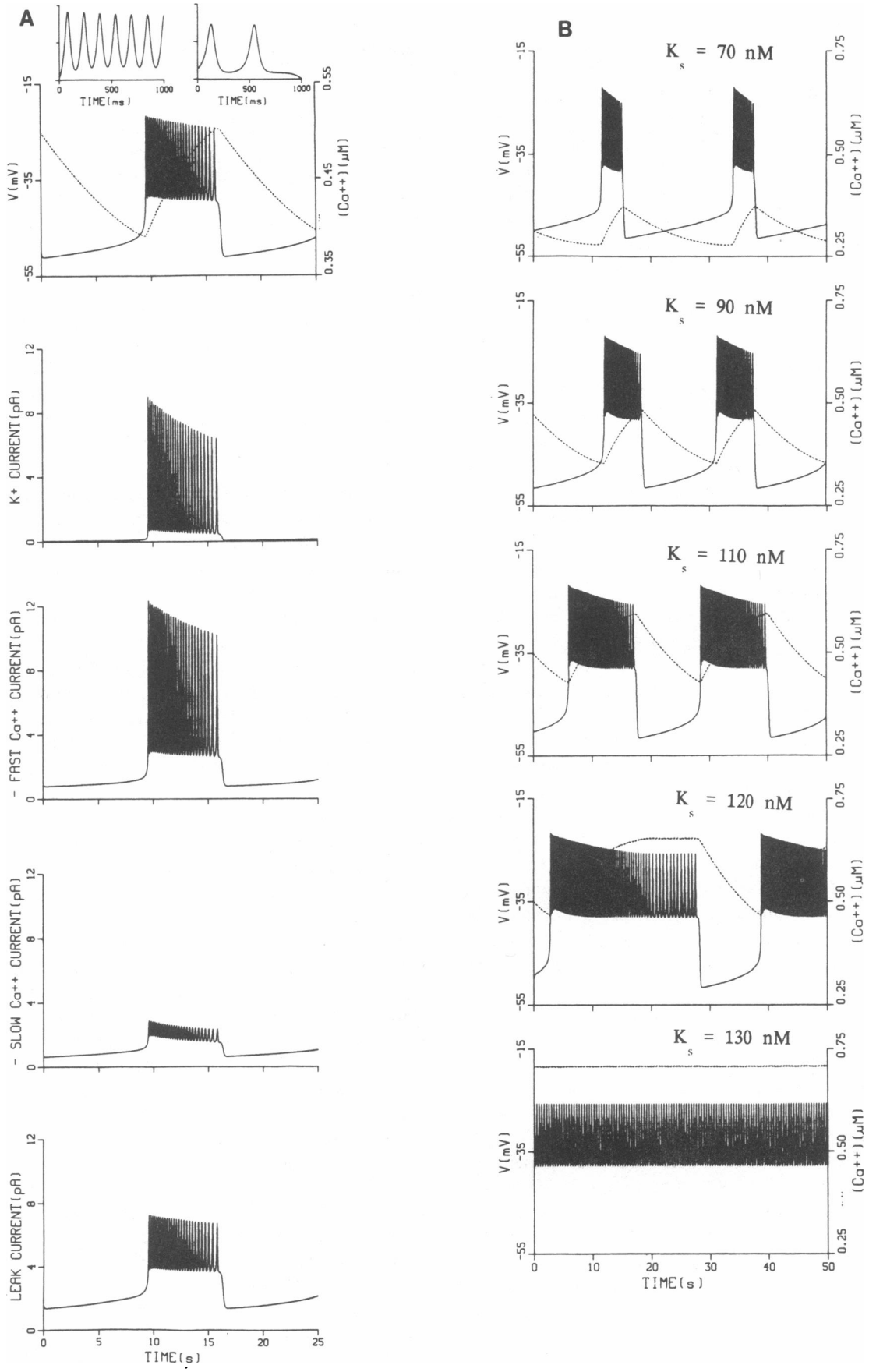

FIGURE 2 (*A*) Simulation of the burst activity of intact β-cell in an islet. Top panel shows the membrane potential V (*solid line*) and intracellular Ca^{2+} concentrations $[Ca^{2+}]_i$ (*dashed line*). Inset shows the initial and final spike shapes. The following three panels show the ionic currents of delayed K^+, fast Ca^{2+}, and slow Ca^{2+} channels, and the bottom panel shows the leak currents. (*B*) The effect of secretagogue on electrical bursting. The effect of secretagogues is modeled by varying the Ca_i dissociation constant K_s of the slow Ca^{2+} channel. From the top trace to bottom, K_s used are 70, 90, 110, 120, and 130 nM.

the similar results as those presented in Figs. 1–4. To test how the size of Δt affects the results, we have used Δt ranging from 0.2 to 0.01 ms, but the results changed little with changing Δt. The burst activities presented in Figs. 2–4 are those in the limit-cycle steady state (i.e., the first 5–10 min of the burst activity are not shown).

In Fig. 1 *A*, we show peak current–voltage relations obtained by applying step potentials to a cell initially resting at −70 mV. The outward K^+ current shown in Fig. 1 *A, top,* is the steady-state current, and it exhibits a linear relation to voltage >-5 mV. The two inward Ca^{2+} currents and the combined current are presented in Fig. 1 *A, bottom.* Reversal of the Ca^{2+} current is seen near +60 mV, which indicates strong inward rectification. The maximum peak (hump) occurs just above −10 mV, and the secondary hump is invisible in the inward (total) current, even though a hump of the fast Ca^{2+} current occurs 22 mV above that of the slow current. It is interesting that, unlike in some neuronal cells (Nowcycky et al., 1985), most of the inward I/V curves in β-cells show a single hump (Satin and Cook, 1985; Findlay and Dunne, 1985; Rorsman and Trube, 1986).

Fig. 1 *B* shows the effect of external calcium concentration on peak inward I/V relations. As the Ca^{2+} concentration is increased from 3 to 12 mM, the inward I_{Ca} grows and the reversal potential becomes more positive. If the independence principle holds, we expect that an *m*-fold increase in $[Ca^{2+}]_o$ results in an *m*-fold rise in the current. The experiment of Rorsman and Trube (1986) shows that a fourfold increase of $[Ca^{2+}]_o$ results in only a 1.6-fold increase in peak inward I/V relations. This suggests ionic flux coupling in a pore of Ca^{2+} channels and a saturation of barrier binding sites (Hille, 1984). Our model assumes that Ca^{2+} ions diffuse from one side to the other through a homogeneous membrane without any interference from other Ca^{2+} ions. Thus, Fig. 1 *B* confirms the independence principle that is assumed in our model. To correct the discrepancy, we need to divide the flux (cf., $I_{Ca,f}$) expression by $1 + [Ca^{2+}]_o/K_M$, where K_M is the Michaelis-Menten constant (Hille, 1984).

Fig. 2 *A, top,* illustrates a mathematically predicted burst pattern in the absence of single-channel stochastic noises. The five differential equations (i.e., V, $[Ca^{2+}]_i$, n, m, s) were solved with the GEAR method. The time course of the membrane potential, V, is presented by the solid line and the intracellular free calcium concentration, $[Ca^{2+}]_i$, is presented by the dashed curve. Note that $[Ca^{2+}]_i$ oscillates between 0.39 μM and 0.54 with the amplitude of 0.15 μM. The spikes shown in the inset reveal that the frequency in the final phase is three times larger than that in the initial phase and that the amplitude is smaller near termination. Such observations have been made in many published β-cell experiments (Atwater et al., 1980; Ribalet and Beigelman, 1980; Cook, 1983). The current components shown in the next four traces reveal that the fast Ca^{2+} current has the largest amplitude and the slow Ca^{2+} the smallest. It is interesting to note that such a small current is enough to transform a spiking cell to a burster. Note also that the slow Ca^{2+} current shows inactivation along the plateau phase, and this inactivation brings about the termination of the plateau phase.

Fig. 2 *B* is to test our hypothesis that some secretagogues and glycolytic metabolites may act as competitive inhibitors of Ca_i and can alter the electrical bursting pattern. The effect of competitive inhibition was modeled by varying K_s. It is quite apparent that our model predicts an increase in the active phase and a decrease in the silent phase as a function of K_s. As a result of this electrical effect, there is a rise in the average $[Ca^{2+}]_i$ level. Above 120 nM, the bursts disappear entirely and only spikes remain. The results on electrical activity are consistent with the burst pattern that is invoked by addition of glucose (Atwater et al., 1980; Ribalet and Beigelman, 1980; Cook, 1984) and pH (Eddlestone and Beigelman, 1983; Pace, 1984).

We have simulated intracellular potential recording from a single isolated β-cell (i.e., Eq. 1 with $g_g = 0$), and the result is presented in Fig. 3, *top*. The Euler method with $\Delta t = 0.02$ ms was used for the computation, and the GGBN (binomial) routine in IMSL was used to generate random numbers. The cell is assumed to contain 1,000 each of the K^+, fast Ca^{2+}, and slow Ca^{2+} channels. Thus, the voltage noise seen in this simulation reflects simultaneous opening-closing events of 3,000 channels. A significant discrepancy between the deterministic model (see Fig. 2 *A*) and the stochastic model lies in the amplitude of $[Ca^{2+}]_i$ oscillation and the nature of bursting. Note that a single cell bursts with very unpredictable periods. Compare the peak of $[Ca^{2+}]_i$ level with that in Fig. 2 *A*. We find that the voltage noise results in a decrease in the amplitude of $[Ca^{2+}]_i$ oscillation, and bursts occur so chaotically that $[Ca^{2+}]_i$ is unable to reach the maximum possible peak (i.e., 0.54 μM).

It is of interest to find out which channel activity contributes the most to the voltage noise seen in Fig. 2 *A, top*. We have studied such an effect by treating the opening events of one type of channel stochastically and the other two deterministically. The voltage noise seen in the second panel is due to the cell containing 1,000 K^+ channels, the third panel 1,000 fast Ca^{2+} channels, and the bottom trace 1,000 slow Ca^{2+} channels. As shown here, 1,000 slow Ca^{2+} channels are enough to suppress most stochastic noises, while the cell needs more than 1,000 fast Ca^{2+} channels to suppress the noise. It is evident that among the three, the K^+ stochastic event contributes the most to the voltage noise. Note that for all three cases, $[Ca^{2+}]_i$ oscillates with a much smaller amplitude and also at a lower level than deterministic $[Ca^{2+}]_i$.

Cells of the islets of Langerhans have been shown to be electrically as well as chemically coupled (Meda et al., 1984; Eddlestone et al., 1984). It would be interesting to know what happens to the voltage noise and the $[Ca^{2+}]_i$

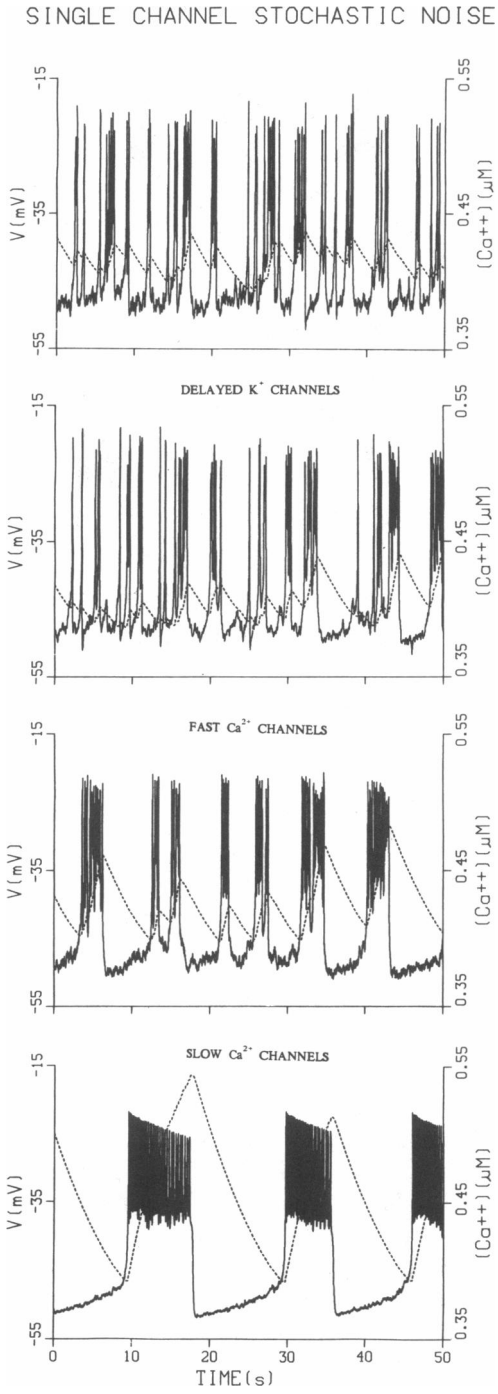

FIGURE 3 Simulation of electrical activity of isolated single β-cell. The cell is assumed to contain 1,000 delayed K^+ channels, 1,000 slow Ca^{2+} channels, and 1,000 fast Ca^{2+} channels. In the second panel, the cell contains 1,000 delayed K^+ channels and an infinitely large number of slow and fast Ca^{2+} channels. Likewise, in the third panel there are 1,000 fast Ca^{2+} channels in the cell, and in the bottom panel there are 1,000 slow Ca^{2+} channels.

level when cells cluster together. The results of increasing the cell number, M, are presented in Fig. 4. To save computation time, we have introduced a few assumptions: (*a*) a single cell contains 1,000 K^+ channels, (*b*) there are an infinitely large number of Ca^{2+} channels (i.e., two types of Ca^{2+} channels were treated deterministically), and (*c*) the β-cells are very, very tightly coupled (i.e., $g_g = \infty$). The last assumption allowed us to treat a multicomplex as if it were a single cell ($g_g = 0$), but with the number of channels increased by a factor of M. The Euler method with Δt = 0.05 ms and the GGBN (binomial) routine were used for the top three traces (1, 10, 50 cells), whereas the Euler method with Δt = 0.02 ms and the GGNQF (normal) routine were used for the next two traces.

When 10 such cells aggregate, irregular bursts develop (see second panel) that resemble those observed by Rorsman and Trube (1986) in a cluster of 70 μm diameter (~80 cells). For an aggregate containing 50 cells or more, (almost) regular bursts develop but the spikes often run irregularly by undershooting and overshooting the plateau level. Note that if there are only 200 delayed rectifier channels in a cell (instead of 1,000 channels), our 10-cell aggregate (second panel) corresponds to a cluster of 50 cells, and the 50-cell aggregate (third panel) corresponds to a cluster of 250 such cells. Note also that as more cells cluster together, the peak of $[Ca^{2+}]_i$ becomes higher.

DISCUSSION

This study represents the first quantitative attempt to search for a clue as to why pancreatic β-cells need to be aggregated tightly and burst in synchrony. To achieve our purpose, we have formulated a stochastic model in which the channels are allowed to open and shut at random, but with opening and closing probabilities based on experimental data. We have found that there is a strong correlation between the size of clusters and the intracellular calcium concentration level. As the size of a cluster grows, (*a*) the voltage becomes less noisy, (*b*) the bursts become more regular, (*c*) the burst period becomes longer, and (*d*) the plateau phase becomes longer. The lengthening of the plateau phase, in turn, gives rise to an increase in the average $[Ca^{2+}]_i$ level. This result is particularly interesting because $[Ca^{2+}]_i$ is implicated in the release of insulin (Scott et al., 1981; Siegel et al., 1983).

The membrane potential is clearly influenced by the random opening and closing of 1,000 delayed rectifier K^+ channels (see Fig. 3). The opening–closing of this channel is enough to cause voltage recording of single cells to be very chaotic. Our theoretical analysis revealed that the fast voltage-gated Ca^{2+} channels can also make the membrane potential somewhat noisy. Because of the channel stochastic event, the spikes appear irregular even though a cluster of 500 cells is tightly coupled together (see Fig. 4). This irregularity, however, is different from the bimodality observed by Soria and Ferrer (1986) in the frequency distribution of the spike amplitude and of the rate of

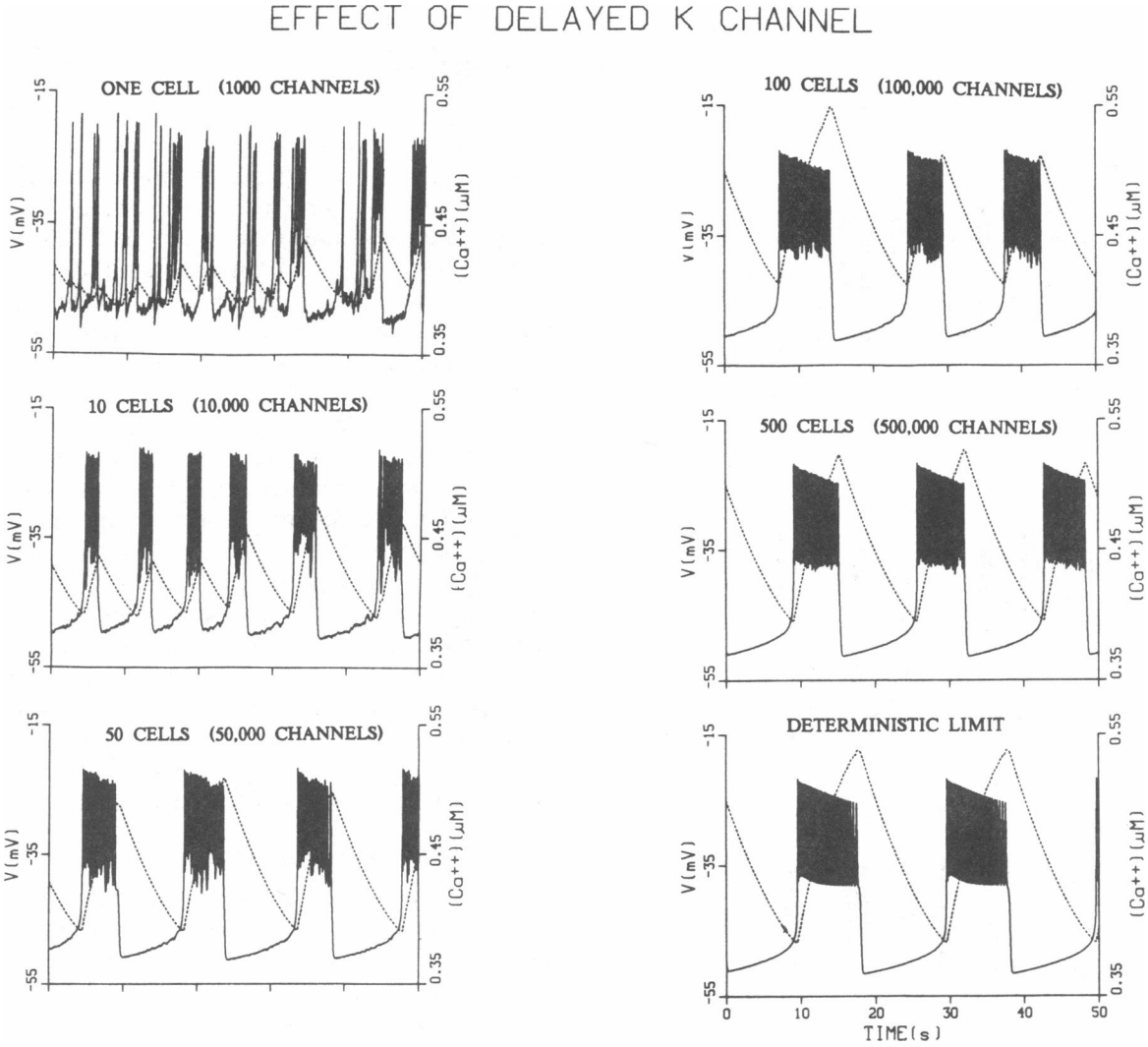

FIGURE 4 Burst activity of a cluster of β-cells as the cluster size (i.e., the number of cells) increases. The noises seen in this figure are due to the open-close event of 1,000 voltage-gated K^+ channels per cell. From the top to the bottom panel, the cluster contains 1, 10, 50, 100, 500, and ∞ cells.

repolarization. As demonstrated by Bangham et al. (1986), a small number of voltage-gated and Ca_i-activated K^+ channels could make regular spikes into very irregular spikes.

In our model, fast voltage-activated Ca^{2+} and delayed rectifier K^+ channels are responsible for spikes, and the slow Ca^{2+} channel is responsible for an underlying slow wave. A small fraction of ATP-sensitive K^+ channels which may still be active in the above subthreshold glucose (Dunne and Petersen, 1986*a* and *b*; Kakei et al., 1986; Rorsman and Trube, 1985; Misler et al., 1966; Himmel and Chay, 1987; Cook et al., 1988) is included in the model as a leak current. The slow wave is achieved by the inhibition of the slow Ca^{2+} channel by the rise in $[Ca^{2+}]_i$. The model predicts that competitive inhibition of the Ca^{2+}-gated channel gives rise to the mean Ca_i level and lengthening of the plateau phase. The competitive inhibition, which is modeled by varing K_s, is not the only way to change the electrical activity. Increasing the Ca^{2+}-ATPase pump activity (k_{Ca}) can also lengthen the plateau phase (Chay, 1987). However, there is one important difference between the effect of k_{Ca} and K_s. The increase in k_{Ca} does not alter the mean $[Ca^{2+}]_i$, whereas the increase in K_s raises the mean $[Ca^{2+}]_i$. This raises an interesting hypothesis on how to separate the electrical activity from the $[Ca^{2+}]_i$ level, as pointed out by Chay (1986 and 1987).

We have not yet studied in detail the sensitivity of the parametric values on the bursting (and therefore how the parameters affect the conclusion). However, it is quite possible to carry out the study using AUTO (Doedel, 1986) and Rinzel's Z-plot analysis (Rinzel, 1985). Based on Rinzel's conclusion (1985) and our preliminary results, we predict that the Z-plot analysis will reveal (*a*) increasing k_{Ca} lengthens the plateau phase but not the mean $[Ca^{2+}]_i$ level; (*b*) increasing K_s not only lengthens the plateau phase but also raises the mean $[Ca^{2+}]_i$; (*c*) increas-

ing f in Eq. 4 increases the burst frequency; (*d*) λ_m and λ_n control the amplitude and frequency of spikes; (*e*) decreasing λ_s transforms a square-wave burster (e.g., β-cell bursting) to a parabolic burster (e.g., R-15 bursting) (Chay and Cook, 1988).

Although our model is very simplistic, it provides valuable information which is not yet obtained experimentally. To summarize, our model predicts that the mean level of $[Ca^{2+}]_i$ rises as the size of a cluster increases (Fig. 4). A competitive inhibitor or activator that alters the Ca_i allosteric site has an ability to influence the electrical activity as well as the mean level of $[Ca^{2+}]_i$ (see Fig. 2 *B*). The electrical activity and the mean $[Ca^{2+}]_i$ can be separated by appropriately varying k_{Ca} and K_s (Chay, 1987). While newer experiments will eventually refine our model, we believe that these predictions are model independent.

We would like to thank Dr. Michael Lambert for his helpful comments.

This work was supported by National Institutes of Health grant R01 HL33905.

REFERENCES

Atwater, I., C. M. Dawson, A. Scott, G. Eddlestone, and E. Rojas. 1980. The nature of the oscillatory behavior in electrical activity of pancreatic β-cell. *In* Biochemistry and Biophysics of the Pancreatic β-Cell. Georg Thieme Verlag, Stuttgart, FRG. 100–107.

Bangham, J. A., P. A. Smith, and P. C. Croghan. 1986. Modeling the β-cell electrical activity. *Adv. Exp. Med. Biol.* 211:265–278.

Chay, T. R. 1986. On the effect of the intracellular calcium-sensitive K^+ channel in the bursting pancreatic β-cell. *Biophys. J.* 50:765–777.

Chay, T. R. 1987. The effect of inactivation of calcium channels by intracellular Ca^{2+} ions in the bursting pancreatic β-cells. *Cell Biophys.* 11:77–90.

Chay, T. R. 1988. Mathematical modeling for the bursting mechanism of insulin secreting β-cell. *Comments Mol. Cell. Biophys.* 4:349–368.

Chay, T. R., and D. L. Cook. 1988. Endogenous bursting patterns in excitable cells. *Math. Biosci.* In press.

Chay, T. R., and H. S. Kang. 1987. Multiple oscillatory states and chaos in the endogenous activity of excitable cells: pancreatic β-cell as an example. *In* Chaos in Biological Systems. H. Degn, A. V. Holden, and L. F. Olsen, editors. Plenum Press, New York. 173–181.

Chay, T. R., and J. Keizer. 1983. Minimal model for membrane oscillations in the pancreatic β-cell. *Biophys. J.* 42:181–190.

Cook, D. L. 1984. Electrical pacemaker mechanisms of pancreatic islet cells. *Fed. Proc.* 43:2368–2372.

Cook, D. L., M. Ikeuchi, and W. Y. Fujimoto, 1984. Lowering of pH_i inhibits Ca^{2+}-activated K^+ channels in pancreatic β-cells. *Nature (Lond.).* 311:269–271.

Cook, D. L., L. S. Satin, M. L. J. Ashford, and C. N. Hales. 1988. ATP-sensitive K-channels in pancreatic B-cells: The "spare channel" hypothesis. *Diabetes.* 37:495–498.

Doedel, E. J. 1986. AUTO86 User Manual. Software for Continuation and Birucation Problems in Ordinary Differential Equations. California Institute of Technology.

Dunne, M. J., and O. H. Petersen. 1986*a*. Intracellular ADP activates K^+ channels that are inhibited by ATP in an insulin-secreting cell line. *FEBS (Fed. Eur. Biochem. Soc.) Lett.* 208:59–62.

Dunne, M. J., and O. H. Petersen. 1986*b*. GTP and GDP activation of K^+ channels that can be inhibited by ATP. *Pfluegers Arch. Eur. J. Physiol.* 407:564–565.

Eckert, R., and J. E. Chad. 1984. Inactivation of Ca channels. *Prog. Biophys. Mol. Biol.* 44:215–267.

Eddlestone, G. T., and P. M. Beigelman. 1983. Pancreatic β-cell electrical activity: the role of anions and the control of pH. *Am. J. Physiol.* 244:C188–C197.

Eddlestone, G. T., A. Goncalves, J. A. Bangham, and E. Rojas. 1984. Electrical coupling between cells in islets of Langerhans from mouse. *J. Membr. Biol.* 77:1–14.

Feller, W. 1968. An Introduction to Probability Theory and Its Applications. Vol. 1. 3rd ed. John Wiley & Sons, Inc., New York. 153–156 and 190–192.

Findlay, I., and M. J. Dunne. 1985. Voltage-activated Ca^{2+} currents in insulin-secreting cells. FEBS *(Fed. Eur. Biochem. Soc.), Lett.* 189:281–285.

Goldman, D. E. 1943. Potential, impedance and rectification in membranes. *J. Gen. Physiol.* 37:37.

Hille, B. 1984. Ionic Channels of Excitable Membrane. Ch. 8 and 11. Sinauer Associates, Inc., Sunderland, MA.

Himmel, D. M., and T. R. Chay. 1987. Theoretical studies on the electrical activity of pancreatic β-cells as a function of glucose. *Biophys. J.* 51:89–107.

Hodgkin, A., and A. F. Huxley. 1952. A quantitative description of membrane current and application to conduction and excitation in nerve. *J. Physiol. (Lond.).* 117:500–544.

Kakei, M., R. P. Kelly, S. J. H. Ashcroft, and F. M. Ashcroft. 1986. The ATP-sensitivity of K^+ channels in B-cells is modulated by ADP. *FEBS (Fed. Eur. Biochem. Soc.) Lett.* 208:63–66.

Kramer, R. H., and R. S. Zucker. 1985. Calcium-induced inactivation of calcium current causes the inter-burst hyperpolarization of Aplysia bursting pace-maker neurones. *J. Physiol. (Lond.).* 362:131–160.

Meda, P., I. Atwater, A. Goncalves, A. Bangham, L. Orci, and E. Rojas. 1984. The topography of electrical synchrony among β-cells in the mouse islet of Langerhans. Quat. J. Exp. Phys. 69:719–735.

Misler, S., L. C. Gillis, K. Gillis, and M. L. McDaniel. 1986. A metabolite-regulated potassium channel in rat pancreatic B cells. *Proc. Natl. Acad. Sci. USA.* 83:7119–7123.

Nowycky, M. C., A. P. Fox, and R. W. Tsien. 1985. Three types of neuronal calcium channel with different calcium agonist sensitivity. *Nature (Lond.).* 316:440–446.

Pace, C. S. 1984. Role of pH as a transduction device in triggering electrical and secretory responses in silent B cells. *Fed. Proc.* 43:2379–2384.

Plonsey, R., and D. G. Fleming. 1969. Bioelectric Phenomena. McGraw-Hill Book Co., New York.

Ribalet, B., and P. M. Beigelman. 1980. Calcium action potentials and potassium permeability activation in pancreatic β-cells. *Am. J. Physiol.* 239:C124–133.

Rinzel, J. 1985. Bursting, oscillations in an excitable model. *In* Lecture Note in Mathematics. A. Dold and B. Eckmann, editors. Springer-Verlag, Berlin.

Rorsman, P., and G. Trube. 1985. Glucose dependent K^+ channels in pancreatic β-cells are regulated by intracellular ATP. *Pfluegers Arch. Eur. J. Physiol.* 405:305–309.

Rorsman, P., and G. Trube. 1986. Calcium and delayed potassium currents in mouse pancreatic β-cells under voltage-clamp conditions. *J. Physiol. (Lond.).* 374:531–550.

Satin, L. S., and D. L. Cook. 1985. Voltage-gated Ca^{2+} current in pancreatic B-cells. *Pfluegers Arch. Eur. J. Physiol.* 404:385–387.

Satin, L. S., and D. L. Cook. 1988: Evidence for two calcium currents in insulin-secreting cells. *Pfluegers Arch. Eur. J. Physiol.* 411:401–409.

Scott, A. M., I. Atwater, and E. Rojas. 1981. A method for the simultaneous measurement of insulin release and B cell membrane potential in single mouse islets of Langerhans. *Diabetologia.* 21:470–475.

Siegel, E. G., C. B. Wollehim, D. Janjic, G. Ribes, and G. W. G. Sharp. 1983. Involvement of Ca^{2+} in the impaired glucose-induced insulin release from islets cultured at low glucose. *Diabetes.* 32:993–1000.

Soria, B., and R. Ferrer. 1986. Graded spike electrogenesis in mouse pancreatic β-cells. *In* Biophysics of the Pancreatic β-Cell. *Adv. Exp. Med. Biol.* 211:235–246.